Metric for the measurement of the quality of complex beams: a theoretical study

Sergiy Kaim,[1] Julien Lumeau,[2] Vadim Smirnov,[3] Boris Zeldovich,[1,*] and Leonid Glebov[1]

[1]*CREOL, The College of Optics and Photonics, University of Central Florida, Orlando, Florida 32816, USA*
[2]*Aix-Marseille Université, CNRS, Centrale Marseille, Institut Fresnel, UMR 7249, 13013 Marseille, France*
[3]*OptiGrate Corp, 562 South Econ Circle, Oviedo, Florida 32765-4311, USA*
**Corresponding author: boris@creol.ucf.edu*

Received November 10, 2014; revised January 14, 2015; accepted January 22, 2015;
posted January 29, 2015 (Doc. ID 226551); published March 12, 2015

We present a theoretical study of various definitions of laser beam width in a given cross section. Quality of the beam is characterized by dimensionless beam propagation products (BPPs) $\Delta x \cdot \Delta\theta_x/\lambda$, which are different for the 21 definitions presented, but are close to 1. Six particular beams are studied in detail. In the process, we had to review the properties for the Fourier transform of various modifications and the relationships between them: physical Fourier transform (PFT), mathematical Fourier transform (MFT), and discrete Fourier transform (DFT). We found an axially symmetric self-MFT function, which may be useful for descriptions of diffraction-quality beams. In the appendices, we illustrate the thesis "the Fourier transform lives on the singularities of the original."

OCIS codes: (120.4800) Optical standards and testing; (070.2465) Finite analogs of Fourier transforms; (070.7345) Wave propagation.
http://dx.doi.org/10.1364/JOSAA.32.000538

1. INTRODUCTION

The problem of characterizing and measuring the transverse quality of a laser beam has a long history in the literature, and specifically, it is worth mentioning a monograph by Siegman [1] and a paper by Siegman [2] as examples. Most laser beams have very small angular divergence θ_x ($\leq 10^{-2}$ rad). Transformation of such beams by lenses without aberrations may separately change $\delta\theta_x$ and the waist radius Δx. However, the product $\Delta x \cdot \Delta\theta_x$ (of dimension meters) is not changed by such transformation, and for almost-diffraction-quality beams, it is of the order of wavelength λ. Particular dimensionless quantity $\Delta x \cdot \Delta\theta_x/\lambda$ depends on the formal definition of Δx and $\Delta\theta_x$ in theoretical discussions of the problem, and it depends on the measuring procedures in an experiment.

One possible definition of $\Delta x \cdot \Delta\theta_x$ is the root mean square, and related to it is the dimensionless parameter M_x^2, which has been adopted as ISO standard [3]:

$$\Delta x_{\mathrm{rms}} = \sqrt{\langle (x - \langle x\rangle)^2\rangle}, \qquad \Delta\theta_{\mathrm{rms}} = \sqrt{\langle (\theta_x - \langle\theta_x\rangle)^2\rangle},$$
$$M_x^2 = (4\pi/\lambda)\cdot \Delta x_{\mathrm{rms}} \cdot \Delta\theta_{\mathrm{rms}}. \tag{1}$$

Separate measurements of M_x^2 and M_y^2 are often necessitated by the not quite axially symmetric character of the beam, including possible astigmatism. The particular coefficient, 4π, is chosen in such a manner that the minimum value of M_x^2 equals 1, and this is achieved for an ideal beam with a perfect Gaussian profile.

It is assumed in Eq. (1) that Δx_{rms} is measured at the z-position of its minimum (at the focal waist in the case of a focused beam), while $\Delta\theta_{\mathrm{rms}}$ is measured in the far-field zone of the beam. Quite often in the experiment, the far-field zone with its angular distribution of intensity $I(\theta_x)$ is substituted by the profile $I_{\mathrm{waist}}(x = F\cdot\theta_x)$ in the focal plane of a positive lens with focal distance F. This often leads to confusion regarding which parameter, Δx_{rms} or $\Delta\theta_{\mathrm{rms}}$, corresponds to the near field and which one is related to the far field. Luckily, this modest confusion in terminology does not result in a change of M_x^2, because as we have already mentioned, the product $\Delta x \cdot \Delta\theta_x$ is invariant under transformation by paraxial optical elements without aberrations.

Many researchers have noted that the quantities Δx_{rms}, $\Delta\theta_{\mathrm{rms}}$ and therefore $M_x^2 = 4\pi\cdot\Delta x_{\mathrm{rms}}\cdot\Delta\theta_{\mathrm{rms}}/\lambda$ put too much emphasis upon distant wings of distributions $I_0(x)$ and $I_1(\theta_x)$, e.g., [4–7]. This includes an experimental paper by Lantigua *et al.* [7].

Our personal preference is for the use of a criterion involving the "width of the slit, containing 85% of total power," and the ratio of the beam propagation product (BPP) to the BPP for an ideal Gaussian beam by the same criterion. The chosen fraction of 85% seems to be reasonable for energy-delivering applications of laser beams. Meanwhile the slit technology is relatively easy to implement in field devices.

Given field $E_0(x,y)$ in the near-field zone, one finds the intensity profile there as $I_0(x,y) = |E_0(x,y)|^2$. Besides that, the angular amplitude profile, i.e., the amplitude profile in the far-field zone, is proportional to

$$G_2(\theta_x,\theta_y) = \frac{1}{2\pi}\iint E_0(x,y)e^{-ik(x\cdot\theta_x + y\cdot\theta_y)}\mathrm{d}x\mathrm{d}y. \tag{2}$$

The resultant angular intensity profile is $I_2(\theta_x,\theta_y) = |G_2(\theta_x,\theta_y)|^2$. In the $(1\mathrm{D}+z)$ case, $E_0(x,y)\equiv E_0(x)$ and

$$G_1(\theta_x) = \frac{1}{\sqrt{2\pi}} \int E_0(x) \exp(-ikx \cdot \theta_x) \mathrm{d}x. \tag{3}$$

Additionally, $I_1(\theta_x) = |G_1(\theta_x)|^2$. Here and below, the wavenumber $k = 2\pi/\lambda$, and λ is the wavelength in the medium of the propagation path (typically in a vacuum).

For that reason, in Section 2 we review three definitions of the Fourier transform (FT): the physical Fourier transform (PFT), the mathematical Fourier transform (MFT), and the discrete Fourier transform (DFT). Specifically, in Section 2B, we discuss the one-dimensional self-MFT functions. In Section 2C, we discuss the DFT and its relationship to PFT and MFT. In Section 2D, we introduce a new axially symmetric self-MFT function based on the 1D self-MFT function $1/\cosh(x\sqrt{\pi/2})$.

In Section 3, we consider 21 quantitatively different definitions of the beam width and produce a calculation table of those widths for 6 different smooth transverse profiles in the near field. We also calculate their far-field profiles. In this manner, we were able to find BPPs for these beams according to the 21 different criteria. The tables of BPPs are compiled with the assumption that one and the same criterion of width (out of the 21 considered) was taken for both the near field and far field. Meanwhile, we provide data from the calculations, which allow one to take one criterion in the near field and another in the far field, and thus arrange for such a compound BPP. Section 4 summarizes the results of this work. In Appendix A we illustrate the thesis "the Fourier transform lives on the singularities of the original." While this thesis is not scientifically new, we failed to find a mathematical presentation of it in textbooks or papers. In Appendix B, we apply DFT for the study of self-MFT functions.

2. FOURIER TRANSFORMS: PHYSICAL, MATHEMATICAL, AND DISCRETE FOURIER TRANSFORMS AND THE SELF-MATHEMATICAL FOURIER TRANSFORM FUNCTION

A. Physical Fourier Transform (PFT)

We start with the FT as it is used in the PFT. Consider the function $f(x)$ of real variable x (for example, of dimensions of Cartesian coordinate $[x] = [\text{meter}]$). This function may have real or complex values. We define the new function $G(q)$ for the new real argument q (of dimensions $[q] = [\text{radian/meter}]$) by

$$G(q) = \frac{A}{\sqrt{2\pi}} \int_{-\infty}^{+\infty} \exp(iqx) f(x) \mathrm{d}x, \tag{4}$$

where $A \neq 0$ is some constant. Then, as it is well known in mathematics, under certain (not very restrictive) conditions, the original function $f(x)$ may be found by inverse Fourier transformation as follows:

$$f(x) = \frac{1}{A\sqrt{2\pi}} \int_{-\infty}^{+\infty} \exp(-iqx) G(q) \mathrm{d}q. \tag{5}$$

Traditional choices of constant A are, for example, $A = 1$, $A = \sqrt{2\pi}$, and $A = 1/\sqrt{2\pi}$, but any $A \neq 0$, even a complex number, does the job. Equation (4) defines the linear operator of the PFT; it maps the space of functions $f(x)$ of argument x onto the space of functions $G(q)$ of a different argument q, dimensions of q being inverse to the dimensions of x: $[q] = [1/x]$. Parseval's theorem claims that

$$|A|^2 \cdot \int_{-\infty}^{+\infty} |f(x)|^2 \mathrm{d}x = \int_{-\infty}^{+\infty} |G(q)|^2 \mathrm{d}q. \tag{6}$$

It looks especially elegant for $A = 1$.

B. Mathematical Fourier Transform (MFT)

If one wants to discuss eigenfunctions of FT, then the FT operator must map space functions $f(y)$ onto itself, $G(y)$. In that case, dimensions $[q \equiv y]$ coincide with dimensions $[1/y]$. In other words, argument x of functions $f(x)$ for the MFT should be dimensionless. All this gives justification to the following definition of the MFT operator as

$$\mathrm{MFT}\{f\}(x) = h(x) = \frac{1}{\sqrt{2\pi}} \int_{-\infty}^{+\infty} \exp(ixx') f(x') \mathrm{d}x'. \tag{7}$$

Parseval's theorem shows that the MFT operator is unitary:

$$\int |h(x)|^2 \mathrm{d}x = \int |f(x')|^2 \mathrm{d}x'. \tag{8}$$

Inverse PFT in Eq. (5) differs (at $A = 1$) from the original PFT in Eq. (4) only by the sign of phase in the exponential. This allows us to conclude that application of the MFT operator to a function $f(x)$ two times returns $f(-x)$:

$$(\mathrm{MFT})^2\{f\}(x) = f(-x). \tag{9}$$

From that one gets

$$(\mathrm{MFT})^4\{f\}(x) = f(x), \quad \text{or} \quad (\mathrm{MFT})^4 = \hat{1}, \tag{10}$$

i.e., the 4th power of the MFT operator is the unit operator. As a result, eigenvalues Λ of the MFT operator satisfy condition $\Lambda^4 = 1$,

$$\mathrm{MFT}\{h\}(x) = \Lambda \cdot h(x), \qquad \Lambda^4 = 1. \tag{11}$$

Thus, there are only four possible eigenvalues of MFT: $\Lambda_0 = 1$, $\Lambda_1 = i$, $\Lambda_2 = -1$, and $\Lambda_3 = -i$ (or $\Lambda_n = i^n$, where $n = 0, 1, 2, 3$).

Differentiation and integration by parts in MFT Eq. (7) allow one to show that if $f(x)$ is an eigenfunction of MFT with eigenvalue Λ_f, i.e., if

$$\mathrm{MFT}\{f\}(x) = \Lambda_f \cdot f(x), \tag{12}$$

then functions

$$g(x) = \left(x - \frac{d}{dx}\right) f(x), \qquad h(x) = \left(x + \frac{d}{dx}\right) f(x) \tag{13}$$

are also eigenfunctions of MFT, and

$$\Lambda_g = i \cdot \Lambda_f, \qquad \Lambda_h = -i \cdot \Lambda_f. \tag{14}$$

Function $g_0(x) = \exp(-x^2/2)$ is a well known eigenfunction of MFT with an eigenvalue $\Lambda_0 = +1$. Moreover, Hermite polynomials $H_n(x)$ multiplied by $g_0(x)$, i.e.,

$$H_n(x)\exp(-x^2/2), \tag{15}$$

up to constant factors, can be produced from $g_0(x)$ by application of the "creation operator" $(x - d/dx)$ sequentially n times. Therefore, they are eigenfunctions of MFT with eigenvalues $\Lambda_n = i^n$.

Another function,

$$c_0(x) = \left[\cosh\left(x\sqrt{\pi/2}\right)\right]^{-1}, \tag{16}$$

is also an eigenfunction of MFT with an eigenvalue $\Lambda_0 = +1$. The main difference between $g_0(x)$ and $c_0(x)$ is in their asymptotic behavior at $|x| \to \infty$: $g_0(x) = \exp(-x^2/2)$ (exact); meanwhile, $c_0(x) \doteq 2\cdot\exp(-|x|\sqrt{\pi/2})$. Functions $\mathrm{const}_g \cdot g_0(x)$ and $\mathrm{const}_c \cdot c_0(x)$ normalized to $\int |f(x)|^2 \mathrm{d}x = 1$ have almost 100% overlapping integrals:

$$\|g_0 c_0\|^2 \equiv \frac{\left[\int_{-\infty}^{+\infty} g_0(x)c_0(x)\mathrm{d}x\right]^2}{\left[\int_{-\infty}^{+\infty} |g_0(y)|^2\mathrm{d}y\right]\cdot\left[\int_{-\infty}^{+\infty} |c_0(z)|^2\mathrm{d}z\right]} = 0.994. \tag{17}$$

Property $(\mathrm{MFT})^4 = \hat{1}$ allows one to construct eigenfunctions of MFT out of an arbitrary function $f(x)$ of the dimensionless argument. For example,

$$f_\beta(x) = f(x) + i^\beta \mathrm{MFT}\{f\}(x) + i^{2\beta}(\mathrm{MFT})^2\{f\}(x) + i^{3\beta}(\mathrm{MFT})^3\{f\}(x) \tag{18}$$

is an eigenfunction of MFT with eigenvalue $\Lambda = i^\beta$, where β is any integer number from 0 to 3. For the case with $\Lambda = +1$, i.e., when $\beta = 0$ is considered, formula of the type in Eq. (18) was suggested in [8,9].

Curious examples of MFT eigenfunctions are

$$r_{\mathrm{even}}(x) = \frac{1}{\sqrt{|x|}}, \qquad r_{\mathrm{odd}}(x) = \frac{x}{|x|}\cdot\frac{1}{\sqrt{|x|}}, \tag{19}$$

with respective eigenvalues $\Lambda_{\mathrm{even}} = +1$, $\Lambda_{\mathrm{odd}} = +i$. However, each of them has a logarithmically divergent normalization integral (both at $|x| \to 0$ and at $|x| \to \infty$).

C. Discrete Fourier Transform (DFT) and Approximation of PFT by DFT

Discrete FT is usually introduced as an approximation for the PFT. Consider function $f(x)$ at the interval $a \le x < a + L$, and for definiteness, let dimensions of x be $[x]$ = [meters]. Let us characterize this function by its values at the set of N equidistant points $n = 0, 1, \ldots, N-1$,

$$x_0 = a, x_1 = a + s_x, \ldots, x_n = a + ns_x, \ldots, x_{N-1} = a + (N-1)s_x; \qquad s_x = L/N. \tag{20}$$

Here, s_x is a step of the x-coordinate. It is convenient to assume that function $f(x)$ is continued outside the interval $a \le x < a + L$ in a periodic manner with period L, so that $f(x) = f(x + L)$. Then, one can consider an extra point $x_{\mathrm{extra}} = a + s_x N \equiv a + L$ with the value $f(a + L) = f(a) \equiv f_0$, which is already accounted for by f_0. The corresponding vector $\vec{f}$ of N-dimensional linear space has components

$$\vec{f} = [f_0 = f(x_0), f_1 = f(x_1), \ldots, f_{N-1} = f(x_{N-1})]. \tag{21}$$

Function $G(q)$ [i.e., PFT from Eq. (4)] may be approximated by a trapezoid formula:

$$G(q) \approx \frac{A}{\sqrt{2\pi}} s_x [0.5 f_0 e^{iqx_0} + f_1 e^{iqx_1} + f_2 e^{iqx_2} + \ldots + f_{N-1}e^{iqx_{N-1}} + 0.5 f(x_{\mathrm{extra}})e^{iqx_{\mathrm{extra}}}]. \tag{22}$$

The periodicity assumption yields $f(x_{\mathrm{extra}}) \equiv f_0$. Evidently, there are only N linear independent values of function $G(q)$ defined by Eq. (22). To express this idea, we can choose to consider N discrete values of argument q:

$$q_0 = 0, q_1 = s_q, q_2 = 2s_q, \ldots, q_{N-1} = (N-1)s_q. \tag{23}$$

The periodicity condition in the x-coordinate with period L may be satisfied if the value of the step s_q in q-space is chosen as $s_q = 2\pi/L$ (of dimensions [radian/meter]). In that case, $f(x_{\mathrm{extra}})e^{iq_m \cdot x_{\mathrm{extra}}} = f_0 e^{iq_m \cdot x_0}$, and the trapezoid approximation for $G(q)$ becomes

$$G_m \equiv G(m\cdot s_q) \equiv G\left(m\cdot\frac{2\pi}{L}\right) \approx \frac{L\cdot A}{N\sqrt{2\pi}}\exp\left(2\pi i\frac{ma}{L}\right)\sum_{n=0}^{N-1} f_n \exp\left(2\pi i\frac{n\cdot m}{N}\right). \tag{24}$$

Vector $\vec{g}$ of N-dimensional linear space is called the DFT of vector $\vec{f}$ from the same space, if its components are defined by

$$g_m = (\mathrm{DFT}\{f\})_m = \frac{1}{\sqrt{N}}\sum_{n=0}^{N-1} f_n \exp\left(2\pi i\frac{n\cdot m}{N}\right). \tag{25}$$

The operator of the DFT is implemented in every widely used mathematical software package like Mathcad, MatLab, Maple, Mathematica, etc. What we were able to formulate here is that the PFT $G(q)$ from Eq. (4) may be approximated by

$$G\left(q_m \equiv \frac{2\pi m}{L}\right) \approx \exp\left(2\pi i\frac{ma}{L}\right)\frac{L\cdot A}{\sqrt{2\pi N}}(\mathrm{DFT}\{f\})_m. \tag{26}$$

Intuitively, it is clear that the DFT of Eq. (25) is a certain approximation of the PFT. What is important is that the particular q_m-dependent coefficient in Eq. (26) expresses the PFT via the DFT.

Remarkable mathematical facts about the operator of the DFT defined by Eq. (25) are as follows: 1) the DFT is an unitary operator in N-dimensional linear space; 2) the inverse DFT operator (IDFT) looks like an approximation of Eq. (5) for the inverse PFT (IPFT), but it is actually an **exact** inverse operator with respect to DFT:

$$f_n = (\mathrm{IDFT}\{\vec{g}\})_n = \frac{1}{\sqrt{N}}\sum_{m=0}^{N-1} g_m \exp\left(-2\pi i\frac{n\cdot m}{N}\right). \tag{27}$$

The proof of this fact uses the following formula for the sum of geometrical progression:

$$\sum_{k=0}^{N-1}\eta^k = [N, \text{if } \eta = 1; (1-\eta^N)/(1-\eta) \text{ otherwise}], \tag{28}$$

where $\eta = \exp[2\pi i(n-m)/N]$.

An additional problem to be considered is that physically both the positive and negative values of q[rad/meter] in Eqs. (4) and (5) are important. At first glance, $q_m = s_q \cdot m = 2\pi m/L$ with $m = 0, 1, \ldots, N-1$ cover positive values of q only. This difficulty can be resolved rather simply. For values $q_{N/2} = N\pi/L$, the exponential factors $\exp(iq_m \cdot x_n) = \exp(iq_m \cdot a) \cdot \exp(i\pi n)$ oscillate versus n as $\exp(i\pi n) \equiv (-1)^n$. This is a manifestation of the failure of discretization of $f(x)$ into $f_n = f(x_n)$. In other words, we expect the PFT of our function $f(x)$ to be negligibly small at q_m with $m \approx N/2$. However, subtracting $Q = 2\pi N/L$ from any of the q_m does not change the exponential factors in the DFT. Indeed, $\exp[i(q_m - Q)x_n] = \exp[i(q_m - Q)a] \cdot \exp[iq_m s_x n] \cdot \exp[-iQs_x n]$. But $\exp[-iQns_x] = \exp(-2\pi in) \equiv 1$. Therefore, one can subtract $Q = 2\pi N/L$ from any q_m without changing the resultant DFT. We can now introduce function

$$\text{phys}(m) = \begin{cases} m, & \text{if } m < N/2 \\ -N + m, & \text{otherwise} \end{cases}, \tag{29}$$

so that $q_m(\text{physical}) = s_q \cdot \text{phys}(m)$ values represent the positive q in the range of $0 \le m < N/2$ and negative $q = -Q + q_m$ in the range of $N/2 \le m \le N-1$.

D. Generation of Eigenfunctions of 2D MFT via Eigenfunctions of 1D MFT

The definition of MFT for functions of two dimensionless variables x, y is a trivial generalization of the 1D case:

$$2D\,\text{MFT}\{f\}(x,y) = \frac{1}{2\pi}\iint_{-\infty}^{\infty} e^{i(xx'+yy')} f(x',y')\mathrm{d}x'\mathrm{d}y'. \tag{30}$$

Consider two eigenfunctions of 1D MFT: $f_1(x)$ and $f_2(x)$, with eigenvalues $\Lambda_1 = (i)^{\beta_1}$ and $\Lambda_2 = (i)^{\beta_2}$, respectively. Functions $f_1(x)$ and $f_2(x)$ may be identical; in that case, $\Lambda_1 \equiv \Lambda_2$. Besides that, $f_1(x)$ and $f_2(x)$ may be different eigenfunctions of MFT with the same or with different eigenvalues Λ_1 and Λ_2. In any of these cases, the factorized function of two dimensionless variables

$$F_{\text{factor}}(x,y) = f_1(x)f_2(y), \qquad \Lambda_{\text{factor}} = \Lambda_1 \cdot \Lambda_2 \tag{31}$$

is an eigenfunction of the unitary 2D MFT operator of Eq. (30), and $\Lambda_{\text{factor}} = \Lambda_1 \cdot \Lambda_2$. The proof of this simple statement is based on factorization of the exponential kernel in the 2D MFT (30) as follows:

$$e^{ix\cdot x' + iy\cdot y'} = e^{ix\cdot x'} \cdot e^{iy\cdot y'}. \tag{32}$$

Besides that, the scalar product $(\mathbf{r}\cdot\mathbf{r}') \equiv xx' + yy'$ in that kernel is invariant with respect to simultaneous rotation of coordinates by arbitrary angle ψ:

$$(x,y)_{\text{new}} = (x,y)\hat{R}, \qquad (x',y')_{\text{new}} = (x',y')\hat{R},$$
$$\hat{R} = \begin{pmatrix} \cos\psi & \sin\psi \\ -\sin\psi & \cos\psi \end{pmatrix}. \tag{33}$$

Therefore, another function,

$$F_{\text{new},\psi}(x,y) = f_1(x_{\text{new}})f_2(y_{\text{new}}) = f_1(x\cos\psi + y\sin\psi)\cdot f_2(-x\sin\psi + y\cos\psi), \tag{34}$$

which generally is not factorized into $h_1(x)\cdot h_2(y)$, is still an eigenfunction of the 2D MFT with $\Lambda_{\text{new}} = \Lambda_1 \cdot \Lambda_2$. Linearity of the 2D MFT operator guarantees that any superposition of such functions with ψ-dependent weight $W(\psi)$,

$$F_{\text{superp}}(x,y) = \int_0^{2\pi} W(\psi)f_1(x\cos\psi + y\sin\psi)f_2(-x\sin\psi + y\cos\psi)\mathrm{d}\psi, \tag{35}$$

is still an eigenfunction of the 2D MFT. Using polar coordinates $x = \rho\cos\varphi, y = \rho\sin\varphi$ in the x,y-plane, one can transform this superposition to

$$F_{\text{superp}}(x,y) = F_{\text{new}}(\rho,\varphi) = \int_0^{2\pi} W(\psi)f_1(\rho\cos(\varphi-\psi))f_2(\rho\sin(\varphi-\psi))\mathrm{d}\psi \tag{36}$$

Let us assume that function $W(\psi)$ is periodic with period 2π, i.e., $W(\psi + 2\pi) = W(\psi)$. Introducing the new variable $\alpha = \varphi - \psi$, one transforms the integral of Eq. (36) up to a factor (-1) into

$$F_{\text{new}}(\rho,\varphi) = -\int_0^{2\pi} W(\varphi+\alpha)\cdot f_1(\rho\cos\alpha)\cdot f_2(\rho\sin\alpha)\mathrm{d}\alpha. \tag{37}$$

A minor problem may arise if the integral in the right-hand side of Eq. (37) turns out, for some or other symmetry reason, to be exactly zero. Then, one gets a function equal to zero identically, which is not interesting, albeit it may formally be considered as an eigenfunction of any linear operator.

Special interest is presented by the case when $W(\psi) = (-1/2\pi)\exp(im\psi)$ to elucidate the rotation symmetry in the (x,y)-plane. Then,

$$F_{\text{new}}(\rho,\varphi) = e^{im\varphi}R_m(\rho),$$
$$R_m(\rho) = \frac{1}{2\pi}\int_0^{2\pi} e^{im\alpha}f_1(\rho\cos\alpha)f_2(\rho\sin\alpha)\mathrm{d}\alpha. \tag{38}$$

We are especially interested in the case of completely axially symmetric ($m = 0$) 2D self-MFT functions:

$$R_0(\rho) = \frac{1}{2\pi}\int_0^{2\pi} f_1(\rho\cos\alpha)f_2(\rho\sin\alpha)\mathrm{d}\alpha. \tag{39}$$

If $f_1(x) = f_2(x) = \exp(-x^2/2)$, then the axially symmetric result is trivial, where $R_0(\rho) = \exp(-\rho^2/2)$.

We were lucky to find another example of a completely symmetric 2D self-MFT function with eigenvalue $\Lambda = +1$:

$$C_{00}(\rho) = \frac{1}{2\pi}\int_0^{2\pi} c_0(\rho\cos\alpha)c_0(\rho\sin\alpha)\mathrm{d}\alpha, \qquad \Lambda = 1, \quad (40)$$

where $c_0(x) = 1/\cosh(x\sqrt{\pi/2})$. A graph of this new function is presented in Fig. 1.

Behavior of this function at small and large ρ (remember that ρ is dimensionless) is as follows:

$$C_{00}(\rho) = 1 - \frac{\pi}{4}\rho^2 + O(\rho^4) \qquad \text{at } \rho \to 0, \quad (41)$$

$$C_{00}(\rho) \doteq \left[4/\left(\rho\cdot\sqrt{\pi/2}\right)\right]\exp\left(-\rho\sqrt{\pi/2}\right) \qquad \text{at } \rho \to 0. \quad (42)$$

Normalized (by $\int_0^\infty |f(x)|^2\rho\mathrm{d}\rho$) function $C_{00}(\rho)$ is mostly very similar to the normalized axially symmetric function $g_0(\rho) = \exp(-\rho^2/2)$. Indeed,

$$\frac{|\int_0^\infty C_{00}(\rho)g_{00}(\rho)\rho\mathrm{d}\rho|^2}{\int_0^\infty [C_{00}(\rho)]^2\rho\mathrm{d}\rho\cdot\int_0^\infty [g_{00}(\rho)]^2\rho\mathrm{d}\rho} = 0.992. \quad (43)$$

However, the asymptotic behavior of $C_{00}(\rho)$ at $\rho \to \infty$ is radically different from that of the Gaussian function. In this respect, $C_{00}(\rho)$ is a better approximation of the radial profile of a single-mode step-profile dielectric fiber with a low V-number.

In particular, consider the axially symmetric mode $\mathrm{LP}_{01}(r)$ of a single-mode fiber with core radius a and V-number

$$V = (2\pi a/\lambda)(n_{\text{core}}^2 - n_{\text{cladding}}^2)^{1/2},$$

where $V = 1.7$, which is well below the threshold $V < 2.4$ for single-mode operation. Our new 2D self-MFT function $C_{00}(\rho = r/u)$ has the best overlapping with $V = 1.7$ normalized mode $\mathrm{LP}_{01}(r)$ at $u = 1.077\cdot a$, and it is equal to

$$F_C = \frac{|\int_0^\infty C_{00}(\rho = r/u)\mathrm{LP}_{01}(r)r\mathrm{d}r|^2}{\int_0^\infty [C_{00}(\rho = r/u)]^2 r\mathrm{d}r\cdot\int_0^\infty [\mathrm{LP}_{01}(r)]^2 r\mathrm{d}r} = 0.9986$$
$$\equiv 1 - 1.14\cdot 10^{-3}. \quad (44)$$

Meanwhile, the same mode has an optimum overlapping integral with the Gaussian function $g_{00}(\rho) = \exp[-(\rho = r/u)^2/2]$ at $u = 1.076\cdot a$; the square of overlapping equals

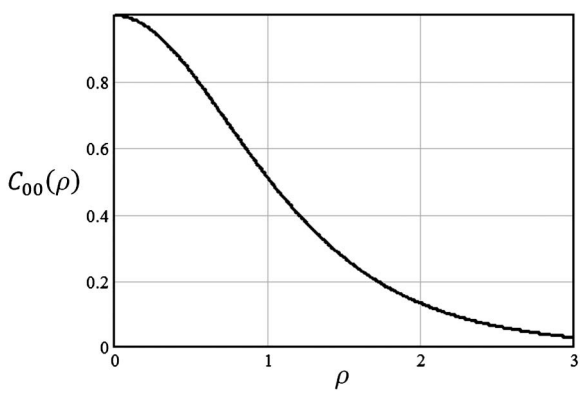

Fig. 1. Self-Fourier transform function $C_{00}(\rho)$.

$$F_g = \frac{|\int_0^\infty g_{00}(\rho = r/u)\mathrm{LP}_{01}(r)r\mathrm{d}r|^2}{\int_0^\infty [g_{00}(\rho = r/u)]^2 r\mathrm{d}r\cdot\int_0^\infty [\mathrm{LP}_{01}(r)]^2 r\mathrm{d}r} = 0.9855$$
$$\equiv 1 - 1.45\cdot 10^{-2}. \quad (45)$$

At $V = 2.4$ (the threshold value of V, below which single mode exists only), the Gaussian function $g_{00}(\rho)$ has some advantages over $C_{00}(\rho)$:

$$F_{g,\text{optimum}} = 1 - 3.3\cdot 10^{-3}, \qquad F_{C,\text{optimum}} = 1 - 5.0\cdot 10^{-3}.$$

However, both approximations are pretty good. A detailed study of the approximation for fundamental modes of a fiber by use of the Gaussian function was done by Marcuse [10], where he considered a variety of smoothed profiles for the fiber refractive index.

3. CALCULATION OF DATA FOR THE BEAM PROPAGATION PRODUCT (BPP) ACCORDING TO 21 POSSIBLE CRITERIA FOR 6 PARTICULAR HIGH-QUALITY BEAMS

Now, we consider numerous possible criteria for the beam width, be it in the near field waist (in units of meters) or in the far field (in units of radians). Below is the list of the 21 criteria that were covered, and these were formulated for quantities of the dimensions [meters]. Similar definitions can be taken for θ_x or for $\theta = (\theta_x^2 + \theta_y^2)^{1/2}$ dimensions [radians].

1. Δx (HWHIM): half-width at the level of half the intensity at maximum.
2. Δx (HWe^{-1}IM): half-width at the level $e^{-1} \equiv 0.368$ of the intensity at maximum.
3. Δx (HWe^{-2}IM): half-width at the level $e^{-2} \equiv 0.135$ of the intensity at maximum.
4. Δx (HW10^{-2}IM): half-width at the level 10^{-2} of the intensity at maximum.
5. r (PIB $f = 0.5$): radius of a circle containing fraction $f = 0.5$ of the total power in the bucket of that radius.
6. r (PIB $f = 0.75$): radius of a circle containing fraction $f = 0.75$ of the total power in the bucket of that radius.
7. r (PIB $f = 0.865$): radius of a circle containing fraction $f = 0.865 = 1 - e^{-2}$ of the total power in the bucket of that radius.
8. r (PIB $f = 0.9$): radius of a circle containing fraction $f = 0.9$ of the total power in the bucket of that radius.
9. r (PIB $f = 0.95$): radius of a circle containing fraction $f = 0.95$ of the total power in the bucket of that radius.
10. r (PIB $f = 0.975$): radius of a circle containing fraction $f = 0.975$ of the total power in the bucket of that radius.
11. r (PIB $f = 0.99$): radius of a circle containing fraction $f = 0.99$ of the total power in the bucket of that radius.
12. s (PIS $f = 0.5$): half-width of the minimum width of the slit containing fraction $f = 0.5$ of the total power in that slit for the total width $2s$.
13. s (PIS $f = 0.75$): half-width of the minimum width of the slit containing fraction $f = 0.75$ of the total power in that slit for the total width $2s$.
14. s (PIS $f = 0.865$): half-width of the minimum width of the slit containing fraction $f = 0.865$ of the total power in that slit for the total width $2s$.

15. s (PIS $f = 0.9$): half-width of the minimum width of the slit containing fraction $f = 0.9$ of the total power in that slit for the total width $2s$.

16. s (PIS $f = 0.95$): half-width of the minimum width of the slit containing fraction $f = 0.95$ of the total power in that slit for the total width $2s$.

17. s (PIS $f = 0.975$): half-width of the minimum width of the slit containing fraction $f = 0.975$ of the total power in that slit for the total width $2s$.

18. s (PIS $f = 0.99$): half-width of the minimum width of the slit containing fraction $f = 0.99$ of the total power in that slit for the total width $2s$.

19. $x_{\mathrm{rms}} = \sqrt{\langle (x - \bar{x})^2 \rangle}$, root mean square of variation for the x-coordinate.

20. $x_1 = \langle |x - \bar{x}| \rangle$, average modulus of variation for the x-coordinate.

21. $x_{0.5} = (\langle |x - \bar{x}|^{1/2} \rangle)^2$, square of the average of the square root for the modulus of the coordinate variation.

We calculated the data for six different profiles of the field in the near-field zone: 1) Gaussian $E(x, y) = \exp[-(x^2 + y^2)/w^2]$; 2) super-Gaussian $E(x, y) = \exp[-(x^2 + y^2)^2/w^4]$; 3) axially symmetric 2D sech profile: self-FT profile found in this work, $E(x, y) = C_{00}(\rho = \sqrt{x^2 + y^2}/u)$; 4) profile of the axially symmetric mode of a single-mode fiber with $V = 2.4$ and of core radius a, $E(x, y) = \mathrm{LP}_{01}(r = \sqrt{x^2 + y^2})$; 5) round top hat profile $E(x, y) = 1$ at $\sqrt{x^2 + y^2} \le w$, $E(x, y) = 0$ otherwise; 6) factorized hyperbolic secant profile, $E(x,y) = c_0(X = x/u)c_0(Y = y/u)$, $c_0(t) = 1/\cosh(t\sqrt{\pi/2})$. The data are presented in Table 1.

Since the table contains dimensionless numbers, clarifications should be made in terms of what units of dimensions of

Table 1. Calculation of Individual Widths of Various Beams According to Different Criteria (See Text)

	Gauss, $E(r) = \exp[-(r/w)^2]$	Super Gauss, $E(r) = \exp[-(r/w)^4]$	2D Sech $C_{00}(r/w = u)$	Fiber Mode $\mathrm{LP}_{01}(r)$, $V = 2.4$	Round Top Hat of Radius w	Factorized 1D Hyperbolic Secant $c_0(x/w = u)$
Δx HWHIM, [width/w]	0.5887	0.7677	0.6930	0.6840	1	0.7032
Δx HWe^{-1}IM, [width/w]	0.7070	0.8409	0.8476	0.8052	1	0.8657
Δx HWe^{-2}IM, [width/w]	1	1	1.2685	1.0699	1	1.3225
Δx HW10^{-2}IM, [width/w]	1.5170	1.2318	2.1956	1.6923	1	2.3882
θ_x HWHIM, angle $\cdot$ (w/λ)	0.1874	0.2447	0.1099	0.1493	0.2572	0.1119
θ_x HWe^{-1}IM, angle $\cdot$ (w/λ)	0.2250	0.2913	0.1345	0.1825	0.3048	0.1378
θ_x HWe^{-2}IM, angle $\cdot$ (w/λ)	0.3183	0.3993	0.2012	0.2724	0.4112	0.2105
θ_x HW10^{-2}IM, angle $\cdot$ (w/λ)	0.4829	0.5499	0.3483	0.4518	0.5442	0.3801
r PIB $f = 0.5$, [width/w]	0.5887	0.5807	0.7830	0.6394	0.7070	0.7848
r PIB $f = 0.75$, [width/w]	0.8326	0.7584	1.1551	0.8893	0.8660	1.1591
r PIB $f = 0.865$, [width/w]	1.0006	0.8641	1.4370	1.0699	0.9299	1.4450
r PIB $f = 0.9$, [width/w]	1.0730	0.9069	1.5677	1.1574	0.9487	1.5765
r PIB $f = 0.95$, [width/w]	1.2239	0.99	1.8547	1.3573	0.9747	1.8686
r PIB $f = 0.975$, [width/w]	1.3581	1.0586	2.1304	1.5559	0.9874	2.1509
r PIB $f = 0.99$, [width/w]	1.5174	1.1349	2.4842	1.8161	0.9950	2.5158
θ PIB $f = 0.5$, angle $\cdot$ (w/λ)	0.1874	0.2327	0.1246	0.1654	0.2654	0.1249
θ PIB $f = 0.75$, angle $\cdot$ (w/λ)	0.2650	0.3237	0.1838	0.2414	0.3917	0.1845
θ PIB $f = 0.865$, angle $\cdot$ (w/λ)	0.3185	0.3838	0.2287	0.2963	0.7766	0.2300
θ PIB $f = 0.9$, angle $\cdot$ (w/λ)	0.3415	0.4095	0.2495	0.3208	0.9063	0.2509
θ PIB $f = 0.95$, angle $\cdot$ (w/λ)	0.3896	0.4638	0.2952	0.3720	1.7802	0.2974
θ PIB $f = 0.975$, angle $\cdot$ (w/λ)	0.4323	0.5203	0.3391	0.4175	2.9031	0.3423
θ PIB $f = 0.99$, angle $\cdot$ (w/λ)	0.4830	0.8080	0.3954	0.4705	5.1887	0.4004
s PIS $f = 0.5$, [width/w]	0.3372	0.3357	0.4488	0.3684	0.4040	0.4383
s PIS $f = 0.75$, [width/w]	0.5752	0.5423	0.7864	0.6220	0.6347	0.7763
s PIS $f = 0.865$, [width/w]	0.7467	0.6727	1.0498	0.8031	0.7607	1.0465
s PIS $f = 0.9$, [width/w]	0.8224	0.7257	1.1724	0.8845	0.8054	1.1747
s PIS $f = 0.95$, [width/w]	0.9800	0.8283	1.4425	1.0652	0.8783	1.4615
s PIS $f = 0.975$, [width/w]	1.1207	0.9121	1.7024	1.2463	0.9237	1.7431
s PIS $f = 0.99$, [width/w]	1.2880	1.0037	2.0371	1.4860	0.9587	2.1117
θ_s PIS $f = 0.5$, angle $\cdot$ (w/λ)	0.1073	0.1335	0.0714	0.0946	0.1590	0.0697
θ_s PIS $f = 0.75$, angle $\cdot$ (w/λ)	0.1831	0.2257	0.1252	0.1647	0.2838	0.1235
θ_s PIS $f = 0.865$, angle $\cdot$ (w/λ)	0.2377	0.2907	0.1671	0.2179	0.4194	0.1665
θ_s PIS $f = 0.9$, angle $\cdot$ (w/λ)	0.2618	0.3190	0.1866	0.2420	0.6093	0.1869
θ_s PIS $f = 0.95$, angle $\cdot$ (w/λ)	0.3119	0.3782	0.2296	0.2935	1.1172	0.2326
θ_s PIS $f = 0.975$, angle $\cdot$ (w/λ)	0.3567	0.4343	0.2709	0.3403	1.9249	0.2774
θ_s PIS $f = 0.99$, angle $\cdot$ (w/λ)	0.4100	0.5308	0.3242	0.3966	3.7706	0.3361
$\langle x^2 \rangle^{\frac{1}{2}}$, meter/$w$	0.5	0.4465	0.7193	0.5509	0.5	0.7236
$\langle \lvert x \rvert \rangle$, meter/$w$	0.3989	0.3701	0.5564	0.4363	0.4244	0.5530
$(\langle \sqrt{\lvert x \rvert} \rangle)^2$, meter/$w$	0.3380	0.3205	0.4641	0.3693	0.3723	0.4586
$\langle \theta_x^2 \rangle^{\frac{1}{2}}$, angle $\cdot$ (w/λ)	0.1591	0.2011	0.1145	0.1474	0.7182	0.1152
$\langle \lvert \theta_x \rvert \rangle$, angle $\cdot$ (w/λ)	0.1270	0.1581	0.0885	0.1154	0.3148	0.0880
$(\langle \sqrt{\lvert \theta_x \rvert} \rangle)^2$, angle $\cdot$ (w/λ)	0.1076	0.1336	0.0739	0.0968	0.2093	0.0730

meters those data are given. For the Gaussian and Super-Gaussian beams, 1 and 2, the data are given in units of traditional notations of w, where $w = \Delta x(\mathrm{HW}e^{-2}\mathrm{IM})$. For the new self-FT function $E(x,y) = C_{00}(\rho = \sqrt{x^2+y^2}/u)$, defined by Eq. (40), the coordinate width is given units u. The parameter u in $C_{00}(\rho = \sqrt{x^2+y^2}/u)$ coincides with the $\Delta x(\mathrm{HW}0.2622\mathrm{IM})$ of the said beam, so that $|C_{00}(\rho = 1)|^2 = 0.2622$, while $|C_{00}(\rho = 0)|^2 = 1$.

For the mode of the step-profile fiber with V-number $V = 2.4$, the data are given in units of core radius a. Finally, for the factorized hyperbolic secant $E(x,y) = c_0(X = x/u)c_0(Y = y/u)$, $c_0(t) = 1/\cosh(t\sqrt{\pi/2})$, parameter u may be considered as $\Delta x(\mathrm{HW}0.2788\mathrm{IM})$.

As for the angular profile corresponding to those beams, their parameters, like $\delta\theta$[radians], are expressed in units (λ/w) for the (i) Gaussian, (ii) super-Gaussian, and (v) round top hat beams; units of (λ/u) were used for the (iii) axially symmetric sech beam and the (vi) factorized sech beam. Finally, for the (iv) LP_{01}-mode of a fiber with V-number $V = 2.4$, the angular width is expressed in units of (λ/a).

The round top hat beam has a well known angular distribution of amplitude and intensity:

$$|G(\theta_x,\theta_y)|^2 = \mathrm{const}\left(\frac{J_1(v)}{v}\right)^2,$$
$$v = \frac{2\pi w}{\lambda}\cdot\sqrt{\theta_x^2+\theta_y^2}, \tag{46}$$

so that the 1st zero of intensity of the so-called "Airy disk" corresponds to $(\theta_x^2+\theta_y^2)^{0.5} = 1.22\lambda/2w$. Power-in-the-bucket fraction for the intensities profile in Eq. (46) is given by

$$f(\theta) = 1 - \left[J_0\left(\frac{2\pi w\theta}{\lambda}\right)\right]^2 - \left[J_1\left(\frac{2\pi w\theta}{\lambda}\right)\right]^2. \tag{47}$$

Here and in Eq. (46), J_0 and J_1 are Bessel functions. Fraction of power-in-the-bucket of the radius $\theta_{\mathrm{Airy}} = 1.22\lambda/(2w)$ is $f(\mathrm{PIB}\,\theta = 1.22\lambda/(2w))$; numerically, it is equal to $f = 1 - (J_0(3.8317))^2 = 0.8378$. Intensity wings of this angular distribution yield logarithmically divergent $\langle\theta_x^2\rangle$. The finite value of θ_x^2 for that table is calculated by truncation of the integral for θ_x^2 at a value of $\theta_{\max} = 10\lambda/w$.

Table 2 contains the BPP values for those six beams: $\Delta\theta\cdot\Delta x/\lambda$ or $\delta\theta\cdot r/\lambda$. In these BPPs, we assumed one and the same criterion (out of 21) for the coordinate size (Δx or r) and for the angular size ($\Delta\theta_x$ or θ). In principle, one can compile $21\times21\times6 = 2646$ products if different criteria are used for the near field and far field; Table 1 contains all the necessary data. Table 3 follows the ideology of Lantigua *et al.* [7], i.e., to divide the BPP of the measured beam by the BPP of the Gaussian beam, which is taken by the same criteria. In Lantigua *et al.* [7], the authors used experimentally measured coordinates and angular widths taken by particular criterion PIS $f = 0.85$ (which is very close to our $0.865 = 1 - e^{-2}$).

The results depicted in Table 3 disprove a deeply entrenched myth that the Gaussian field profile has the best BPP. This myth is definitely valid for the root mean square criterion (i.e., M_x^2 criterion), but not necessarily for other criteria. Particular boxes where other beams show BPPs smaller than Gaussian are emphasized by the bold font. However, the "advantage" of the other beams is not very strong.

Observing the data from Tables 1–3, we can see that the six beams of essentially diffraction quality all have a BPP of about 1. Therefore, the particular choice of criteria should depend on the task for which the beam is intended in a particular application. Experimental work by Lantigua *et al.* [7] used (PIS $f = 0.85$) criteria for both the near-field and far-field zones. Power-in-the-slit is easier to measure in an experiment than PIB, especially power-in-the-circular bucket. However, PIB may be more important in a number of applications for laser beams.

Table 2. Beam Propagation Products for Various Near-Field Profiles $E(x,y)$ (See Text)

$r\cdot\theta/\lambda$, $s\cdot\theta_x/\lambda$, M	Gauss, $E(r) = \exp[-(r/w)^2]$	Super Gauss, $E(r) = \exp[-(r/w)^4]$	2D Sech $C_{00}(r)$	Fiber Mode $\mathrm{LP}_{01}(r)$, $V = 2.4$	Round Top Hat	Factorized 1D Hyperbolic Secant
HWHIM	0.1103	0.1878	0.0764	0.1021	0.2572	0.0787
$\mathrm{HW}e^{-1}\mathrm{IM}$	0.1591	0.2450	0.1143	0.1469	0.3048	0.1193
$\mathrm{HW}e^{-2}\mathrm{IM}$	0.3183	0.3993	0.2561	0.2915	0.4112	0.2783
$\mathrm{HW}10^{-2}\mathrm{IM}$	0.7329	0.6774	0.7672	0.7645	0.5443	0.9078
PIB $f = 0.5$	0.1103	0.1351	0.0976	0.1058	0.1877	0.0980
PIB $f = 0.75$	0.2206	0.2455	0.2123	0.2147	0.3392	0.2138
PIB $f = 0.865$	0.3183	0.3316	0.3286	0.3170	0.7221	0.3323
PIB $f = 0.9$	0.3665	0.3714	0.3911	0.3713	0.8598	0.3955
PIB $f = 0.95$	0.4768	0.4591	0.5475	0.505	1.7352	0.5557
PIB $f = 0.975$	0.5871	0.5508	0.7223	0.6496	2.8666	0.7363
PIB $f = 0.99$	0.7329	0.9169	0.9822	0.8544	5.1627	1.0073
PIS $f = 0.5$	0.0362	0.0448	0.0320	0.0348	0.0642	0.0306
PIS $f = 0.75$	0.1053	0.1224	0.0985	0.1025	0.1801	0.0959
PIS $f = 0.865$	0.1775	0.1955	0.1754	0.1750	0.3191	0.1743
PIS $f = 0.9$	0.2153	0.2315	0.2188	0.2141	0.4907	0.2196
PIS $f = 0.95$	0.3057	0.3133	0.3312	0.3126	0.9812	0.3400
PIS $f = 0.975$	0.3998	0.3962	0.4613	0.4241	1.7781	0.4836
PIS $f = 0.99$	0.5280	0.5327	0.6605	0.5893	3.6150	0.7097
$M_x^2 = (4\pi/\lambda)\cdot\sqrt{\langle x^2\rangle\langle\theta_x^2\rangle}$	1	$2/\sqrt{\pi} = 1.1281$	1.0349	1.0182	4.5771 (∞)	1.0472
$M_1 = (4\pi/\lambda)\cdot\langle\lvert x\rvert\rangle\langle\lvert\theta_x\rvert\rangle$	0.6366	0.7349	0.6192	0.6326	1.6784	0.6117
$M_{0.5} = (4\pi/\lambda)\langle\sqrt{\lvert x\rvert}\rangle^2\langle\sqrt{\lvert\theta_x\rvert}\rangle^2$	0.4569	0.5381	0.4308	0.4493	0.9787	0.4206

Table 3. Ratios of Beam Propagation Products for the Beams under Study to Those of the Gaussian Beam[a]

$r\cdot\theta/\lambda$, $s\cdot\theta_x/\lambda$, M	Gauss, $E(r)=\exp[-(r/w)^2]$	Super Gauss, $E(r)=\exp[-(r/w)^4]$	2D Sech $C_{00}(r)$	Fiber Mode $LP_{01}(r)$, $V=2.4$	Round Top Hat	Factorized 1D Hyperbolic Secant
HWHIM	1	1.7026	**0.6927**	**0.9257**	2.3318	**0.7135**
HWe^{-1}IM	1	1.5399	**0.7184**	**0.9233**	1.9158	**0.7497**
HWe^{-2}IM	1	1.2545	**0.8046**	**0.9158**	1.2919	**0.8744**
HW10^{-2}IM	1	**0.9243**	1.0468	1.0431	**0.7427**	1.2392
PIB $f=0.5$	1	1.2248	**0.8849**	**0.9592**	1.7017	**0.8887**
PIB $f=0.75$	1	1.1129	**0.9624**	**0.9733**	1.5376	**0.9693**
PIB $f=0.865$	1	1.0418	1.0324	**0.9959**	2.2686	1.0440
PIB $f=0.9$	1	1.0134	1.0671	1.0131	2.346	1.0793
PIB $f=0.95$	1	**0.9629**	1.1483	1.0591	3.6393	1.1655
PIB $f=0.975$	1	**0.9382**	1.2303	1.1065	4.8826	1.2541
PIB $f=0.99$	1	1.2511	1.3402	1.1658	7.0442	1.3744
PIS $f=0.5$	1	1.2376	**0.884**	**0.9613**	1.7735	**0.8445**
PIS $f=0.75$	1	1.1624	**0.9354**	**0.9734**	1.7104	**0.9108**
PIS $f=0.865$	1	1.1014	**0.9882**	**0.9859**	1.7977	**0.9820**
PIS $f=0.9$	1	1.0752	1.0163	**0.9944**	2.2791	1.0200
PIS $f=0.95$	1	1.0249	1.0834	1.0226	3.2097	1.1121
PIS $f=0.975$	1	**0.991**	1.1538	1.0608	4.4475	1.2095
PIS $f=0.99$	1	1.0089	1.2509	1.1161	6.8466	1.3440
$M_x^2=(4\pi/\lambda)\cdot\sqrt{\langle x^2\rangle\langle\theta_x^2\rangle}$	1	1.1281	1.0349	1.0182	4.5771 (∞)	1.0472
$M_1=(4\pi/\lambda)\cdot\langle\lvert x\rvert\rangle\langle\lvert\theta_x\rvert\rangle$	1	1.1544	**0.9727**	**0.9937**	2.6365	**0.9609**
$M_{0.5}=(4\pi/\lambda)\langle\sqrt{\lvert x\rvert}\rangle^2\langle\sqrt{\lvert\theta_x\rvert}\rangle^2$	1	1.1777	**0.9429**	**0.9834**	2.142	**0.9205**

[a]We have emphasized in bold font the particular cells of the table where the ratios are smaller than 1. We can see that the completely symmetric self-Fourier transformed beam $\boldsymbol{C}_{00}(\boldsymbol{\rho})$ based on hyperbolic secant functions [Eq. (40)] yields certain advantages over the Gaussian beam, albeit for a limited number of criteria. Actually, the advantages are rather modest at about 4% to 30%, depending on the particular criterion.

4. CONCLUSION

We discussed 21 different criteria for the width of a laser beam. Those criteria are applicable both for the near-field waist, where the width Δx or r has dimensions of [meters], and for the far-field zone, where the width $\Delta\theta_x$ or θ has dimensions of [radians]. Since the field amplitude in the far-field zone is a FT of Eqs. (2) or (3) of the profile of the field in the waist, we provide necessary information about the properties of the FT using the PFT approach [Eq. (4)], the MFT approach [Eq. (7)], and the computationally convenient DFT [Eq. (25)]. We established simple quantitative relationships between the PFT, MFT, and DFT.

That information has allowed us to find an axially symmetric eigenfunction of MFT Eq. (40).

Using Fourier transformation, we were able to find the values of Δx and $\Delta\theta_x$ (or r and θ) according to 21 criteria for slightly different beams of almost diffraction quality.

In our opinion, the use of particular criterion involving the "width of the slit, containing 85% of total power," constitutes a reasonable compromise between following the energy budget of the beam, on one hand, and the suppression of unimportant wings of intensity distribution and measurement noise, on the other hand. Such a technique has been demonstrated in recent physical experiments [7]. Dividing the BPP to that of the ideal Gaussian beam provides the quality parameter, which is close to well known M_x^2-criterion, but without the drawbacks of the latter.

Results of our theoretical work show that taking some other diffraction-quality beam as etalon for comparison (instead of the Gaussian) does not introduce much of a change.

In Appendices A and B, we further illustrate the important properties of the PFT and the connections between the DFT and MFT.

APPENDIX A: NOTION OF EDGE WAVES—ASYMPTOTIC BEHAVIOR OF FOURIER TRANSFORM AT LARGE "q"

The Fraunhofer zone, i.e., far-field amplitude, may be presented in the following form (see Goodman [11,12] and Gbur [13]):

$$E(X,Y,Z)=\frac{k}{2\pi iZ}\exp(ik|\mathbf{R}|)G_2(q_x,q_y),$$
$$G_2(\mathbf{q})=\iint \mathrm{d}x'\mathrm{d}y'E(z'=0,\mathbf{r}')\exp(-i\mathbf{q}\cdot\mathbf{r}'). \quad \text{(A1)}$$

Here, $(q_x,q_y)=(\theta_x,\theta_y)(2\pi/\lambda)=(X/Z,Y/Z)(2\pi/\lambda)$, and we assume $\exp(-i\omega t)$ time dependence. This means that the angular-dependent diffraction amplitude is a 2D-Fourier transform of the original field.

Appendix A is devoted to discussion of the properties of the 1D-Fourier transform,

$$G(q)=G_2(q_x=q,q_y=0)=\int_{-\infty}^{+\infty}E(x)\exp(-iqx)\mathrm{d}x. \quad \text{(A2)}$$

Here,

$$E(x)=\int_{-\infty}^{+\infty}E(x,y')\mathrm{d}y'. \quad \text{(A3)}$$

We assume that $E(x\to-\infty)=E(x\to+\infty)=0$. Consider the question of asymptotic behavior of the diffraction amplitude, i.e., 1D-Fourier transformation (A2) at large values of $|q|$ [the actual small parameter for this asymptotic expansion is $(|q|\Delta x)^{-1}$]. With this aim in mind, one can identically transform $A(q)$ from (A2) to

$$G(q) \equiv \frac{i}{q}\int_{-\infty}^{+\infty} E(x)\frac{d}{dx}\exp(-iqx)\mathrm{d}x. \tag{A4}$$

Integration of this formula by parts, with account of $E(x \to -\infty) = E(x \to +\infty) = 0$, yields

$$G(q) \equiv -\frac{i}{q}\int_{-\infty}^{+\infty} \exp(-iqx)\frac{d}{dx}E(x)\mathrm{d}x. \tag{A5}$$

If function $E(x)$ contains several discrete steps at points $x = a$, $x = b$, with the magnitude of steps $\Delta E_a = E(x \to a + \varepsilon) - E(x \to a - \varepsilon)$, $\varepsilon \to +0$, etc., then the function dE/dx contains a corresponding number of δ-functions:

$$\frac{dE}{dx} = \Delta E_a \cdot \delta(x-a) + \Delta E_b \cdot \delta(x-b) + \ldots + \left(\frac{dE}{dx}\right)_{\text{extracted}}. \tag{A6}$$

Here, $(dE/dx)_{\text{extracted}}$ denotes the part of the (dE/dx) function with extracted $\Delta E_j \cdot \delta(x - x_j)$ terms. As a result, $G(q)$ takes the form

$$G(q) = -\frac{i}{q}[\Delta E_a e^{-iqa} + \Delta E_b e^{-iqb} + \ldots] - \frac{i}{q}\int_{-\infty}^{+\infty} e^{-iqx}\left(\frac{dE}{dx}\right)_{\text{extracted}}\mathrm{d}x. \tag{A7}$$

Under several applications of the same procedure to $(dE/dx)_{\text{extracted}}$, one gets the asymptotic expansion of Fourier transform amplitude $G(q)$ in the form

$$G(q) = \left(-\frac{i}{q}\right)[\Delta E_a e^{-iqa} + \Delta E_b e^{-iqb} + \ldots] + \left(-\frac{i}{q}\right)^2\left[\Delta\left(\frac{dE}{dx}\right)_a e^{-iqa} + \Delta\left(\frac{dE}{dx}\right)_b e^{-iqb} + \ldots\right] + \left(-\frac{i}{q}\right)^3\left[\Delta\left(\frac{d^2E}{dx^2}\right)_a e^{-iqa} + \Delta\left(\frac{d^2E}{dx^2}\right)_b e^{-iqb} + \ldots\right] + \ldots. \tag{A8}$$

Surprisingly, we have not seen an analog of expansion Eq. (A8) in any mathematical textbook, albeit qualified people definitely do know this result. Citing Professor M. V. Berry and late Professor V. I. Arnold, "This result is well known to those, who know well", though they used this phrase on another occasion.

There are several separate corollaries of the result for Eq. (A8). Consider the function $E(x)$, which has zero limits at $x \to \pm\infty$ by itself, and all its derivates have the same property. Then,

1) If $E(x)$ has a finite number of steps (discontinuities), then

$$G(q) = \left(-\frac{i}{q}\right)[\Delta E_a e^{-iqa} + \Delta E_b e^{-iqb} + \ldots] + o\left(\frac{1}{q}\right), \tag{A9}$$

i.e., $G(q)$ decreases as $(1/q)$ at $|q| \to \infty$, with the particular coefficient given by Eq. (A9). Graphs in Fig. 2 illustrate qualitatively the structure of functions $E(x)$, $\Sigma\Delta_j\delta(x - x_j) +$ $(dE/dx)_{\text{extracted}}$, as if $E(x)$ were a real function. In actual applications, $E(x)$ may be complex-valued.

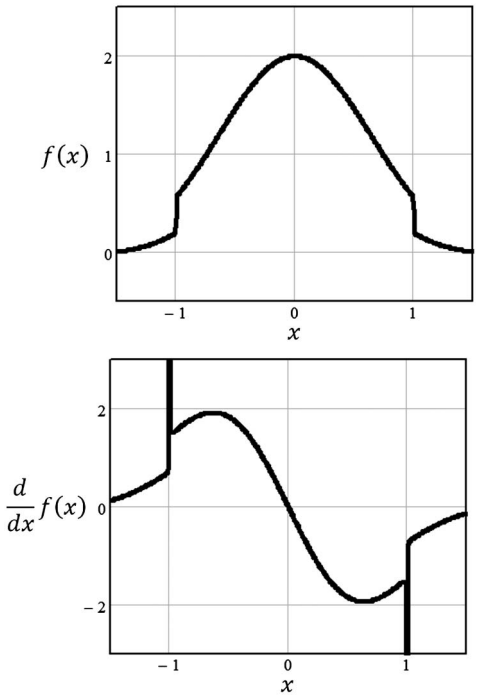

Fig. 2. Example of a function possessing steps and the derivative of that function with δ-type singularities.

2) If $E(x)$ is continuous by itself, but has several discrete steps for the derivative, then

$$G(q) \doteq \left(-\frac{i}{q}\right)^2\left[\Delta\left(\frac{dE}{dx}\right)_a e^{-iqa} + \Delta\left(\frac{dE}{dx}\right)_b e^{-iqb} + \ldots\right]. \tag{A10}$$

3) If the function $E(x)$ and its derivatives [including the 1st, 2nd, …, up to the $(N-1)$st] are continuous, then

$$G(q) \doteq \left(-\frac{i}{q}\right)^{N+1}\left[\Delta\left(\frac{d^NE(x)}{dx^N}\right)_a e^{-iqa} + \ldots\right]. \tag{A11}$$

4) If the function $E(x)$ and ALL its derivatives are continuous, then $G(q)$ at $|q| \to \infty$ goes down faster than any power of $|q|$.

A physical reason for amplitude $E(x)$ to have discontinuity at the integration plane is the presence of sharp, dark edges of aperture; these edges limit the passage of the beam. The corresponding terms in $G(q)$ are "edge waves," which are emitted in the process of diffraction of the incident wave upon that edge; compare this to the exact theory of Fresnel diffraction by a semi-infinite plane [14]. The contribution of steps for the field derivative may be considered as resulting from diffraction by the edge of the transparent refractive prism or as a contribution from the sharp corner in an aperture.

Consider an interesting example of the function $E(x) = \exp(-|x|/a)$. It is continuous by itself, but has a step in the derivative, and as a result

$$\frac{dE}{dx} = -\frac{1}{a}\frac{x}{|x|}E(x); \qquad \frac{d^2E}{dx^2} = -\frac{2}{a}\delta(x-0) + \left(\frac{1}{a}\right)^2 E(x); \ldots. \tag{A12}$$

In this way one can write

$$\frac{d^{2k}E}{dx^{2k}} = -\frac{2}{a}\delta(x-0)\frac{1}{a^{2k-2}} + \left(\frac{1}{a}\right)^{2k}E(x),$$
$$G(q) = -2a\sum_{k=0}^{\infty}\left(-\frac{1}{(qa)^2}\right)^k = \frac{2a}{1+(qa)^2}. \qquad \text{(A13)}$$

So, the summation of the asymptotic series in Eq. (A8) yields an exact Lorentzian profile of $G(q)$.

The general statement "the Fourier transform lives on the singularities of the original" is valid even for the infinitely smooth Lorentzian original,

$$E(x) = \frac{1}{1+(x/b)^2}, \qquad \text{(A14)}$$

if one is allowed to consider singularities $x = ib$ and $x = -ib$ in the complex plane $x = \mathrm{Re}(x) + i\,\mathrm{Im}(x)$. Indeed, for this function $E(x)$, contour integration in the complex plane is elementary and yields

$$G(q) = \begin{cases} (\pi b)\exp[-iq(+ib)] \text{ for } q > 0, \\ (\pi b)\exp[-iq(-ib)] \text{ for } q < 0, \end{cases}$$

i.e.,

$$G(q) = (\pi b)\exp(-b|q|), \qquad \text{(A15)}$$

which 1) is the exact result and 2) is in agreement with the general ideology of Eq. (A8): "the Fourier transform lives on the singularities of the original."

Similar observations can be made for $E(x) = 1/\cosh(x/c)$, with singularities at $x = \pm i\cdot c\cdot\pi\cdot(n+1/2)$, $n = 0, 1, 2, \ldots$. Indeed, in that case

$$E(x) = \frac{1}{\cosh(x/c)} \to G(q) = \frac{c\pi}{\cosh(qc\pi/2)}, \qquad \text{(A16)}$$

and the asymptotic behavior of $A(q)$ at large $|q|$ is

$$G(q) \doteq 2\pi c\,\exp(-|q|c\pi/2), \qquad \text{(A17)}$$

due to contributions of those poles $x_n = \pm i\pi c(n+1/2)$ of the original, which are closest to the real axis ($n = 0$), and in complete accord with the ideology of Eq. (A8). Moreover, the traditional way of exactly calculating the Fourier transform for $E(x)$ from Eq. (A16) is to elucidate the contributions of those two poles.

We also were able to find a function $f_c(x)$ with the following curious asymptotic behavior of MFT at $|x| \to \infty$. Its MFT decreases faster than any power of $|x|^{-n}$, but slower than $\exp(-\gamma|x|)$ with any $\gamma > 0$. To possess such an unusual property, $f_c(x)$ must have singularity (or several of them) on the real axis in the plane, $\mathrm{Im}(x = x' + ix'') = 0$. However, this singularity should not have discontinuity of $f_c(x)$ or of any derivative $d^N f/dx^N$ of finite order N. Here is an example of such a function:

$$f_c(x) = \left[1 - \exp\left(-\frac{1}{|x|}\right)\right]\exp\left(-\sqrt[4]{(1+x^2)}\sqrt{2}\right). \qquad \text{(A18)}$$

By itself, $f_c(x)$ is not an eigenfunction of MFT. However, we were able to check numerically that application of procedure Eq. (18) from the main text to $f_c(x)$ transforms it to an MFT eigenfunction, while preserving property

$$f_{\text{self-MFT}}(x) = \exp\left\{-c\cdot|x|^{\frac{1}{2}} + O[\ln|x|]\right\} \text{ at } x \to \infty, \qquad c \approx 1.6. \qquad \text{(A19)}$$

However, the resultant self-MFT function at $|x| \gtrsim 1$ had oscillations (changes of sign).

APPENDIX B: STUDY OF EIGENFUNCTIONS OF MFT VIA DFT

The discussion of eigenfunctions of the MFT operator acting upon functions of the dimensionless argument x requires a large symmetric interval $-L/2 < x < L/2$, i.e., $a = -L/2$, and L is also dimensionless. Using DFT as an approximation of MFT means that the step in the x-coordinate is the same as the step in the q-coordinate. Recalling that $s_x = L/N$ and $s_q = 2\pi/L$, we obtain from the requirement $s_q = s_x$ the relationship $2\pi/L = L/N$, that is,

$$L = \sqrt{2\pi N}, \qquad s_x = s_q = \sqrt{2\pi/N}. \qquad \text{(B1)}$$

So the length L of the x-interval $-L/2 < x < L/2$ is a dimensionless number in that application of DFT, and it grows as $\sqrt{2\pi N}$ with the growth of N. For example, $N = 2^{10} = 1024$ yields an interval of dimensionless length $L \approx 80$ and step $s_x = s_q \approx 0.08$; and for $N = 2^{20} = 1,048,576$ one gets $L \approx 2.6\cdot 10^3$ and $s_x = s_q \approx 2.5\cdot 10^{-3}$. A larger N yields a better approximation of MFT by DFT. In its turn, approximation of

$$h(x) = \mathrm{MFT}\{f\}(x) = \frac{1}{\sqrt{2\pi}}\int f(x')\exp(ixx')\mathrm{d}x \qquad \text{(B2)}$$

via DFT is made by the following formulae:

$$f_n = f(-0.5L + n\cdot L/N), \qquad y_m = \frac{L}{N}\cdot\mathrm{phys}(m),$$
$$h(y_m) = (-1)^m(\mathrm{DFT}\{f\})_m. \qquad \text{(B3)}$$

The difference between $\Lambda\cdot f_n$ and $(-1)^n\cdot(\mathrm{DFT}\{f\})_{\mathrm{phys}(n)+N/2}$ characterizes the error in the hypothetical relationship

$$f(x) = ? = \Lambda\frac{1}{\sqrt{2\pi}}\int_{-\infty}^{+\infty} f(x')\exp(ixx')\mathrm{d}x. \qquad \text{(B4)}$$

We verified this procedure with functions $g_0(x) = \exp(-x^2/2)$ and $c_0(x) = 1/\cosh(x\sqrt{\pi/2})$, both corresponding to eigenvalues of $\Lambda_0 = 1$, and function $g_1(x) = 0.5(x - d/dx)g_0(x) \equiv xg_0(x)$, corresponding to an eigenvalue of $\Lambda_1 = +i$. Even for a very small N, $N = 32$, and $L \approx 14$ and $s \approx 0.4$, the maximum modulus of error under that procedure was 10^{-11} for $g_0(x)$, 10^{-10} for $xg_0(x)$, and 10^{-4} for $c_0(x)$. For $N = 512$, $L \approx 56$, and $s \approx 0.11$, the maximum modulus of error was less than or about 10^{-15} for all of these three functions.

ACKNOWLEDGMENTS

The work was supported by Navy Contract N68335-12-C-0239 and HEL JTO, ARO contract W911NF-10-1-0441.

REFERENCES

1. A. E. Siegman, *Lasers* (University Science Books, 1986).
2. A. E. Siegman, "How to (maybe) measure laser beam quality," in *DPSS (Diode Pumped Solid State) Lasers: Applications and Issues*, M. Dowley, ed. (Optical Society of America, 1998), Vol. **17**, paper MQ1.
3. ISO Standard 11146, "Lasers and laser-related equipment—Test methods for laser beam widths, divergence angles and beam propagation ratios" (2005).
4. J. M. Slater and B. Edwards, "Characterization of high-power lasers," Proc. SPIE **7686**, 76860W (2010).
5. S. Ruschin, E. Yaakobi, and E. Shekel, "Gaussian content as a laser beam quality parameter," Appl. Opt. **50**, 4376–4381 (2011).
6. H. C. Miller, "A laser beam quality definition based on induced temperature rise," Opt. Express **20**, 28819–28828 (2012).
7. C. Lantigua, J. Lumeau, V. Smirnov, and L. Glebov, "Metric for the measurement of laser power delivery to a target," Appl. Opt., submitted.
8. A. Lohmann and D. Mendlovic, "Self-Fourier objects and other self-transform objects," J. Opt. Soc. Am. A **9**, 2009–2012 (1992).
9. M. J. Caola, "Self-Fourier functions," J. Phys. A **24**, L1143–L1144 (1991).
10. D. Marcuse, "Gaussian approximation of the fundamental modes of graded-index fiber," J. Opt. Soc. Am. **68**, 103–109 (1978).
11. J. Goodman, *Introduction to Fourier Optics*, 3rd ed. (Roberts & Company, 2004).
12. J. Goodman, *Speckle Phenomena in Optics* (Roberts and Company, 2010).
13. G. J. Gbur, *Mathematical Methods for Optical Physics and Engineering* (Cambridge University, 2011).
14. L. D. Landau, E. M. Lifshitz, and L. P. Pitaevskii, *Electrodynamics of Continuous Media*, 2nd ed. (Pergamon, 1984), Chap. 95.